Detailed Comparative Analysis of the Catalytic Mechanisms of β-*N*-Acetylglucosaminidases from Families 3 and 20 of Glycoside Hydrolases

David J. Vocadlo‡ and Stephen G. Withers*

Department of Chemistry, University of British Columbia, 2036 Main Mall, Vancouver, British Columbia V6T 1Z1, Canada

Received June 12, 2005; Revised Manuscript Received July 20, 2005

ABSTRACT: β-*N*-Acetylglucosaminidases are commonly occurring enzymes involved in the degradation of polysaccharides and glycoconjugates containing *N*-acetylglucosamine residues. Such enzymes have been classified into glycoside hydrolase families 3 and 20 and are believed to follow distinct chemical mechanisms. Family 3 enzymes are thought to follow a standard retaining mechanism involving a covalent glycosyl enzyme intermediate while family 20 enzymes carry out a substrate-assisted mechanism involving the transient formation of an enzyme-sequestered oxazoline or oxazolinium ion intermediate. Detailed mechanistic analysis of representatives of these two families provides support for these mechanisms as well as detailed insights into transition state structure. α-Secondary deuterium kinetic isotope effects of $k_H/k_D = 1.07$ and 1.10 for *Streptomyces plicatus* β-hexosaminidase (SpHex) and *Vibrio furnisii* β-*N*-acetylglucosaminidase (ExoII) respectively indicate transition states with oxocarbenium ion character in each case. Brønsted plots for hydrolysis of a series of aryl hexosaminides are quite different in the two cases. For SpHex a large degree of proton donation is suggested by the relatively low value of β_{lg} (−0.29) on k_{cat}/K_m, compared with a β_{lg} of −0.79 for ExoII. Most significantly the Taft plots derived from kinetic parameters for a series of *p*-nitrophenyl *N*-acyl glucosaminides bearing differing levels of fluorine substitution in the *N*-acyl group are completely different. A very strong dependence (slope = −1.29) is seen for SpHex, indicating direct nucleophilic participation by the acetamide, while essentially no dependence (0.07) is seen for ExoII, suggesting that the acetamide plays purely a binding role. Taken together these data provide unprecedented insight into enzymatic glycosyl transfer mechanisms wherein the structures of both the nucleophile and the leaving group are systematically varied.

2-Acetamido-2-deoxy-β-D-glycopyranosides are naturally occurring glycosides found within many of the glycoconjugates and oligosaccharides that are present in an extremely wide variety of organisms ranging from microbes to humans. Unsurprisingly, given their abundance in nature, there are several classes of enzymes comprising both hydrolases and lyases that have evolved to cleave glycosidic linkages involving this saccharide residue. The glycoside hydrolases are particularly abundant and have been classified into many different families of enzymes on the basis of structural and primary sequence similarities. Members of each family have similar three-dimensional structures and use similar catalytic mechanisms. Interestingly, two distinct enzyme-catalyzed hydrolytic mechanisms to cleave the β-glycosidic linkage of 2-acetamido-2-deoxy-β-D-glycopyranosides have evolved in nature. Excellent examples of these two mechanistic classes are the *exo*-β-*N*-acetylglucosaminidases from families 3 and 20 of the glycoside hydrolases (For the family classification system of glycoside hydrolases see: Couthino, P. M., and Henrissat, B. (1999) Carbohydrate-Active Enzyme server at http://afmb.cnrs-mrs.fr/CAZY (*1*, *2*)), which are functionally related in that they both catalyze the release of terminal 2-acetamido-2-deoxy-β-D-glycopyranosides from glycoconjugates, yet are known to use differing catalytic mechanisms (*3*−*7*).

exo-β-*N*-Acetylglucosaminidases from family 3 use a catalytic mechanism involving the formation and breakdown of a covalent α-glycosyl enzyme intermediate (Figure 1, path A) formed on an aspartate residue (*3*). Such a mechanism has been found to operate for the very large majority of retaining β-glycosidases, although in some cases the intermediate forms a covalent linkage to the enzyme through a glutamate or tyrosine residue (*8*−*13*). In the first step of the reaction, the formation of the intermediate, departure of the aglycon leaving group is typically facilitated by a general acid/base catalytic residue which, in the ground-state Michaelis complex, donates a hydrogen bond to the glycosidic oxygen. In the second step of the reaction, the breakdown of the intermediate, this same residue acts as a general base, enhancing the nucleophilicity of a water molecule poised near the anomeric center. This water attacks the anomeric center, displacing the enzymatic nucleophile, with the net result being the formation of the hemiacetal product with retained stereochemistry.

The enzymes from family 20 of glycoside hydrolases, however, are generally held to use a catalytic mechanism involving substrate assistance from the 2-acetamido group of the substrate (Figure 1, path B). Chemical precedent for this reaction has long been known from small molecule studies of the acid-catalyzed hydrolysis of aryl *N*-acetylglucosaminides (*14*−*17*). Early investigations, with isolated

* To whom correspondence should be addressed. E-mail: withers@chem.ubc.ca. Tel: 604 822 3402. Fax: 604 822 8869.

‡ Current address: Department of Chemistry, Simon Fraser University, 8888 University Drive, Burnaby, British Columbia, V5A 1S6, Canada.

10.1021/bi051121k CCC: $30.25
Published on Web 08/27/2005

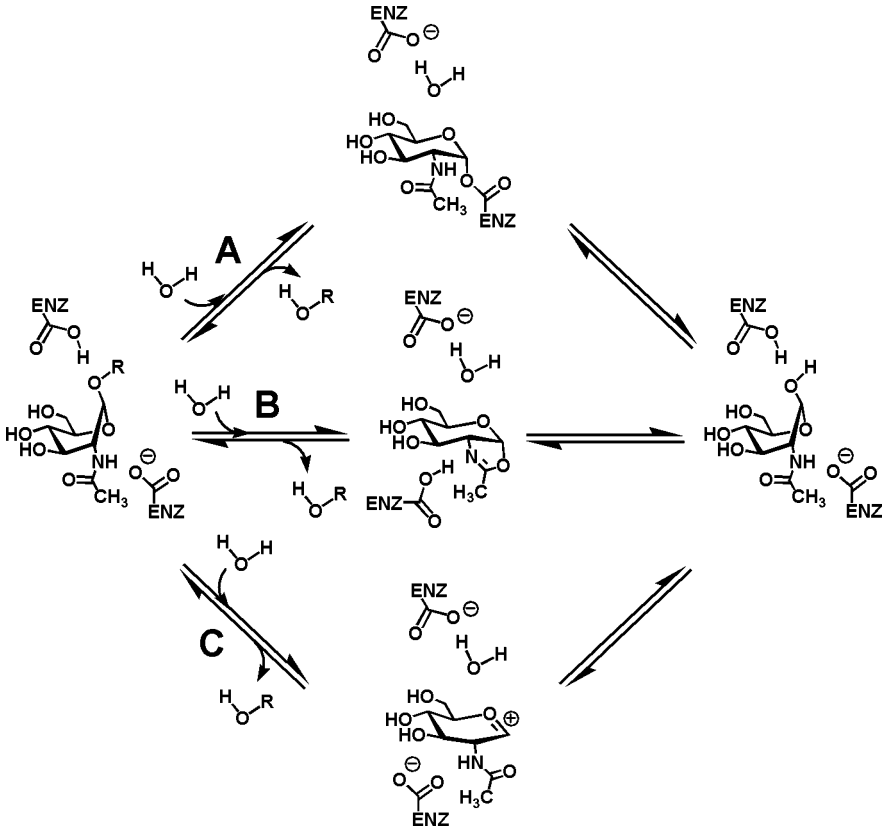

FIGURE 1: The apparent distinction in the catalytic mechanisms of these two classes of *β-N*-acetylglucosaminidase rests in the identity of the nucleophile. The family 3 *β-N*-acetylglucosaminidases use an anionic enzymic carboxylate group as the nucleophile (path A) to form a covalent glycosyl enzyme intermediate. For the family 20 *β-N*-acetylglucosaminidases the 2-acetamido group of the substrate acts as nucleophile (path B) to form a bicyclic oxazoline or oxazolinium ion intermediate. A third alternative has been proposed for the family 20 *β-N*-acetylglucosaminidases involving the formation of an oxocarbenium ion intermediate stabilized by the acetamido group (path C).

Scheme 1: Synthesis of 1-{^{2}H}-pNPGlcNAc[a]

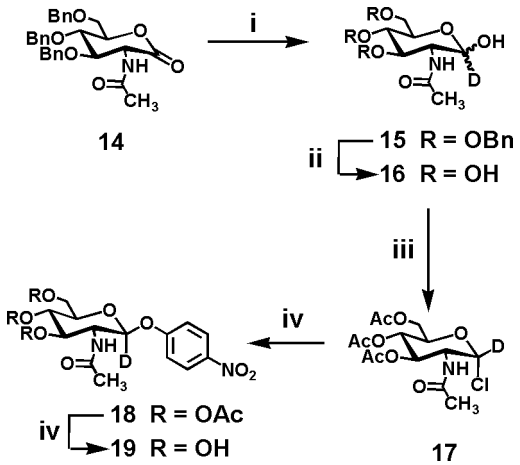

[a] (i) D_2O, $NaBD_4$, THF, 82%; (ii) Pd−C, H_2, EtOAc, MeOH, 88%; (iii) HCl, AcCl, 0 °C → rt; (iv) pNP, Bu_4NHSO_4, CH_2Cl_2, 1 M NaOH, 73% over two steps; (v) (a) NaOMe, MeOH, (b) Amberlite IR-120 (H^+) resin, 78%.

enzymes of unknown sequence, have also provided reasonable evidence supporting such a mechanism (*18*−*20*). More recently, substrate-assisted catalysis has been convincingly shown to operate in family 20 of glycoside hydrolases through both enzyme kinetics studies (*5*, *7*, *21*) and structural studies (*4*, *6*, *22*, *23*).

In the substrate-assisted catalytic mechanism, the carbonyl of the 2-acetamido group acts as a nucleophile to displace the aglycon leaving group with the net result being the formation of a bicyclic oxazoline or oxazolinium ion intermediate (Figure 1, path B). The nucleophilicity of the amide moiety is enhanced by a critically important catalytic residue that hydrogen bonds directly with the amide proton. This critically important residue may act as a general acid/base catalytic residue, deprotonating the acetamido group, or it may act to polarize the amide bond and stabilize a putative oxazolinium ion intermediate (*21*, *24*). In the second step of the reaction a molecule of water attacks the anomeric center, breaking down the oxazoline ring to generate the hemiacetal product with retained stereochemistry (*6*, *25*). In both steps of the reaction a general acid/base catalytic residue acts in a manner analogous to that of the general acid/base catalytic residue seen in the classical double displacement mechanism. An alternative proposal, invoking the formation of an oxocarbenium ion intermediate stabilized by the acetamido group that shields the bottom face of the saccharide ring (Figure 1, path C), has also been proposed on the basis of structural studies of a family 20 enzyme from *Serratia marcescens* (*26*). This proposal, however, lacks experimental support.

Despite the growing interest in glycoside hydrolases as tools for biotechnology applications, detailed mechanistic studies have not been carried out on *β-N*-acetylglucosaminidases of known primary sequence. Because the family 3 and 20 *β-N*-acetylglucosaminidases have evolved to carry out the same function using catalytic mechanisms that clearly differ in the nature of the catalytic nucleophile, we were interested in determining what the mechanistic similarities and differ-

ences between these two families might be. Here we describe a detailed comparative analysis and elucidate the detailed catalytic mechanism of the family 20 β-*N*-acetylglucosaminidase from *Streptomyces plicatus* (SpHex)[1] (*27*) and the family 3 β-*N*-acetylglucosaminidase from *Vibrio furnisii* (ExoII) (*28*).

RESULTS AND DISCUSSION

Requirement for the Acetamido Group. Both ExoII (*28*) and the *S. marcescens* homologue of SpHex (*7*) have been reported to have an absolute requirement for the 2-acetamido group of their substrates. The family 3 β-*N*-acetylglucosaminidases, however, are found within a family of enzymes containing, for example, β-xylosidases and β-glucosidases that process substrates bearing a hydroxyl group in place of a 2-acetamido substituent. Given that this family of enzymes contains such functionally diverse glycosidases, we were interested in establishing whether the acetamido group is required only for substrate recognition rather than more directly in fulfilling a key role in transition state stabilization.

To reevaluate the reported requirement for the 2-acetamido group of substrates for these two enzymes, we assayed 2,4-dinitrophenyl β-D-glucopyranoside (2,4DNPG) as a substrate for both ExoII and SpHex. Because the family 20 enzymes use the 2-acetamido group in catalysis, we expect that a glucoside, even one bearing an excellent leaving group such as 2,4-dinitrophenol, should not be cleaved by SpHex. Conversely, for ExoII, which uses an enzymic nucleophile, the enzyme may well have detectable activity on 2,4DNPG if the 2-acetamido group does not fulfill an essential catalytic role.

As expected, when SpHex (0.2 mg/mL) was incubated overnight with 20 mM 2,4DNPG, no significant activity above that arising from spontaneous hydrolysis could be detected. However, when ExoII was incubated with 2,-4DNPG, significant enzymatic activity was observed. This last observation differs from the results of Chitlaru and Roseman, who could not detect any glucosidase activity (*28*), perhaps because they were not using a highly reactive substrate bearing as activated a leaving group as 2,4-dinitrophenol. Regardless, the Michaelis−Menten parameters for the ExoII-catalyzed hydrolysis of 2,4DNPG could be measured conveniently by continuous assay over five minutes (Figure 2, $k_{cat}/K_m = 0.030 \pm 0.003$ mM^{-1} s^{-1}, $k_{cat} = 0.009 \pm 0.001$ s^{-1}, $K_m = 0.31 \pm 0.02$ mM for substrate concentrations up to 4 mM). This k_{cat} value is approximately 1200-fold lower than that found for 2,3DNPGlcNAc ($k_{cat}/K_m = 130 \pm 10$ mM^{-1} s^{-1}, $k_{cat} = 10.8 \pm 0.2$ s^{-1}, $K_m = 0.09 \pm 0.01$ mM). For retaining glycosidases plots with the shape found in Figure 2 commonly indicate that the second step of the reaction is rate determining and that by increasing the substrate concentration a second molecule of substrate intercepts the glycosyl enzyme intermediate thereby increasing its rate of breakdown. This sequence of events is known as transglycosylation and occurs at elevated substrate concentrations. Thus, the shape of the plot in Figure 2 suggests that the rate-determining step in the ExoII-catalyzed hydrolysis of 2,4DNPG is deglycosylation. Presumably, the very good leaving group makes the first step, glycosylation, faster than the second step. The low K_m value for 2,4DNPG is consistent with such an interpretation as it seems unlikely that a glucoside would have the same affinity as the glucosaminide substrate. The low K_m can most likely be ascribed to the consequence of accumulation of the glycosyl enzyme intermediate. For 2,3DNPGlcNAc, the rate-determining step is also believed to be the deglycosylation step (vide infra). The 1200-fold difference in k_{cat} values for these two substrates therefore underscores an important, yet not vital, role of the acetamido group in stabilizing the second transition state of the family 3 β-*N*-acetylglucosaminidase-catalyzed reaction. Indeed these effects are reminiscent of those found with other retaining glycosidases in which the 2-substituent, typically a hydroxyl, is removed. Enzyme−substrate interactions at the 2-position have been shown to be particularly important for transition state binding (*10*). This finding of some residual activity toward substrates bearing a 2-hydroxyl substituent perhaps reflects their relatively recent evolution from ancestral β-glucosidases. Conversely, these results support the critical requirement of the acetamido group in catalysis by family 20 β-*N*-acetylglucosaminidases.

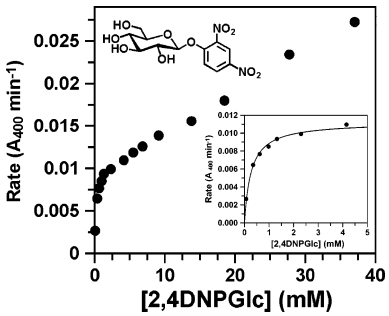

FIGURE 2: Michaelis−Menten plot of the hydrolysis of 2,4DNPG by ExoII. Inset: Region of low 2,4DNPG concentration showing apparent Michaelian saturation kinetics. The chemical structure of 2,4DNPG (**13**) is shown.

Electronic Requirement for the 2-Acetamido Group. Even though it is clear that the acetamido group is involved in catalysis for both enzymes, the extent of involvement in the transition states for catalysis by each enzyme is unknown. Indeed, little is known about the extent of nucleophilic participation of the catalytic nucleophile in retaining glycosidases. This lack of knowledge stems, in part, from the fact that mutagenesis of the enzymic nucleophile allows only the natural set of amino acids to be introduced unless extraordinary measures are taken. For the family 20 *N*-acetylglucosaminidases studied here, however, chemical

[1] Abbreviations: SpHex, *Streptomyces plicatus* β-hexosaminidase; ExoII, *Vibrio furnisii* β-*N*-acetylglucosaminidase; 2,4DNPG, 2,4-dinitrophenyl β-D-glucopyranoside; pNPGlcNAc, *p*-nitrophenyl 2-acetamido-2-deoxy-β-D-glucopyranoside; $pNPGlcNAc_F$, *p*-nitrophenyl 2-fluoroacetamido-2-deoxy-β-D-glucopyranoside; $pNPGlcNAc_{F2}$, *p*-nitrophenyl 2-difluoroacetamido-2-deoxy-β-D-glucopyranoside; $pNPGlcNAc_{F3}$, *p*-nitrophenyl 2-trifluoroacetamido-2-deoxy-β-D-glucopyranoside; 2,3DNPGlcNAc, 2,3-dinitrophenyl 2-acetamido-2-deoxy-β-D-glucopyranoside; 3,5DNPGlcNAc, 3,5-dinitrophenyl 2-acetamido-2-deoxy-β-D-glucopyranoside; pNHAcGlcNAc, *p*-acetamidophenyl 2-acetamido-2-deoxy-β-D-glucopyranoside; mNHAcGlcNAc, *m*-acetamidophenyl 2-acetamido-2-deoxy-β-D-glucopyranoside; mNPGlcNAc, *m*-nitrophenyl 2-acetamido-2-deoxy-β-D-glucopyranoside; MuGlcNAc, 4-methylumbelliferyl 2-acetamido-2-deoxy-β-D-glucopyranoside; PGlcNAc, phenyl 2-acetamido-2-deoxy-β-D-glucopyranoside; $^{\alpha-D}(V/K)_{KIE}$, secondary α-deuterium kinetic isotope effect on V_{max}/K_m; $^{\alpha-D}(V)_{KIE}$, secondary α-deuterium kinetic isotope effect on V_{max}; BSA, bovine serum albumin.

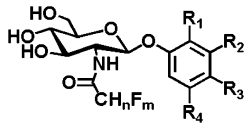

FIGURE 3: Structure of *N*-acyl substituted glucosaminides used in this study.

Table 1: β-*N*-Acetylglucosaminidase-Catalyzed Hydrolysis of Fluoro-Substituted *p*-Nitrophenyl 2-Acetamido-2-deoxy-β-D-glucosides

substrate	σ^* [a]	enzyme	K_m (mM)	k_{cat} (s^{-1})	k_{cat}/K_m (s^{-1} mM^{-1})
pNPGlcNAc	0.0	ExoII	0.73 ± 0.03	3.20 ± 0.04	4.4 ± 0.2
(**1**)		SpHex	0.050 ± 0.004	185 ± 3	3700 ± 350
pNPGlcNAcF	0.8	ExoII	0.68 ± 0.04	3.4 ± 0.2	5.0 ± 0.3
(**2**)		SpHex	0.55 ± 0.02	390 ± 40	720 ± 80
$pNPGlcNAcF_2$	2.0	ExoII	0.33 ± 0.01	2.04 ± 0.02	6.2 ± 0.1
(**3**)		SpHex	0.66 ± 0.02	39 ± 1	59 ± 2
$pNPGlcNAcF_3$	2.8	ExoII	0.138 ± 0.007	0.9 ± 0.1	7 ± 1
(**4**)		SpHex	1.7 ± 0.2	0.95 ± 0.04	0.6 ± 0.1

[a] σ^* is the Taft parameter, values of which were obtained from Hansch and Leo (*52*).

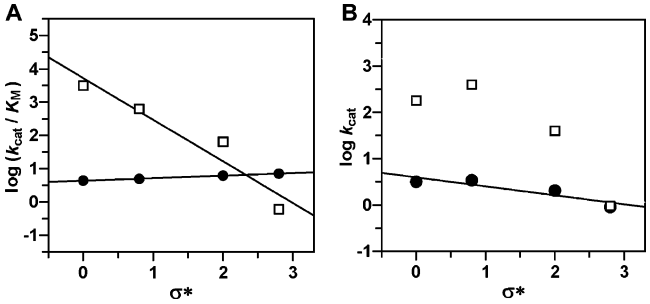

FIGURE 4: Substituent analysis of the ExoII and SpHex β-*N*-acetylglucosaminidase-catalyzed hydrolysis of a series of fluoroacetamido derivatives. (A) Plot of $\log(k_{cat}/K_m)$ against σ^*. (B) Plot of $\log(k_{cat})$ against σ^*. In each plot the filled circles (●) are the data for ExoII and open squares (□) for SpHex. The data and σ^* values used are tabulated in Table 1.

synthesis enables the acetamido group to be altered in order to evaluate the electronic effects of systematically modifying this nucleophile.

To address the electronic requirements of ExoII and SpHex for the acetamido substituent for catalysis we prepared the same series of *p*-nitrophenyl 2-deoxy-2-fluoroacetamido-β-D-glucoside substrates as Yamamoto (*19*, *29*) and Jones (*18*). Increasing levels of substitution of fluorine for hydrogen on the acetamido group decrease the basicity of the carbonyl oxygen nucleophile, making this group a poorer nucleophile. Analysis of pNPGlcNAc, pNPGlcNAcF, $pNPGlcNAcF_2$, and $pNPGlcNAcF_3$ as substrates of both enzymes reveals significant differences in the processing of these substrates by ExoII and SpHex (Figure 3; Table 1). Indeed, increasing fluorine substitution has little effect on the Michaelis−Menten parameters for ExoII while for SpHex a dramatic effect is seen. The data in Table 1 can be represented graphically in a Taft-like free energy relationship. By plotting the log of the first (k_{cat}) and second order (k_{cat}/K_m) rate constants against the Taft parameters for methyl, monofluoromethyl, difluoromethyl, and trifluoromethyl we obtain the relationships shown in Figure 4.

Scatter in free energy relationships of log k_{cat} values may be attributable to differences in ground state binding within the Michaelis complex because the value of k_{cat} is governed by the magnitude of the largest energy barrier from any stable enzyme−substrate or enzyme−intermediate complex to the subsequent transition state. An alternative explanation is that the data may not be scattered, but may represent a biphasic plot indicating that the rate-determining step for SpHex varies depending on the extent of fluorine substitution of the substrate. Increasing the extent of fluorine substitution is expected to make the acetamido group both a worse nucleophile, in the first step of the reaction, and a better leaving group, in the second step of the reaction, with the 2-fold effect of slowing down the cyclization step and accelerating the ring-opening step. As the ring-opening step is rate limiting for pNPGlcNAc (vide infra), it seems reasonable to suppose that the cyclization step may become rate determining for $pNPGlcNAcF_2$ and/or $pNPGlcNAcF_3$. Despite these potential complications, several important points can be made on the basis of the data outlined in Table 1 and Figure 4.

First, as expected, the two enzymes have greatly differing requirements for the 2-acetamido group and enzymes from each family can be readily and rapidly distinguished using these substrates. Second, increasing substitution with fluorine at the methyl group does not exert a significant electronic effect on the transition state for the ExoII-catalyzed hydrolysis of these substrates ($\rho^*_{k_{cat}} = -0.17$ and $\rho^*_{k_{cat}/K_m} = 0.07$). Indeed, there is little effect on k_{cat} or on K_m as can be seen from Table 1. In conjunction with the results of the experiments using 2,4DNPG it appears that the amide functionality is an important, but not critically important, component of catalysis by ExoII probably contributing to transition state binding. Third, Jones and Kosman, using pNPGlcNAc, $pNPGlcNAcF_2$, and $pNPGlcNAcF_3$ as substrates for *Aspergillus niger* β-*N*-acetylglucosaminidase, determined from their three point correlation a slope of -1.41 (*18*); others have determined a slope of -1.0 for human β-hexosaminidase (*30*) and estimated a value of -0.6 for *Aspergillus oryzae* β-*N*-acetylglucosaminidase using a less rigorous strategy (*19*). In these studies the slope is generally a sum of an electronic contribution, ρ^*, which is the Taft parameter associated with the electronic properties of the substituent and a steric contribution, δ, that is associated with the bulk of the substituent; however, these electronic and steric contributions cannot be dissected using the current strategy. The slope observed for the family 20 SpHex, -1.29, is consistent with the values observed for these other enzymes and suggests that the *A. niger* enzyme studied by Jones and Kosman is a member of family 20 of glycoside hydrolases. The marked deleterious effect of including increasing fluorine substitution suggests that in family 20 enzymes there is significant involvement of the acetamido group in the transition state, likely as a nucleophile. Fourth, we can hypothesize that the acetamido group is interacting with a positively charged center in the transition state of the SpHex-catalyzed reaction, since a steep negative correlation in Taft analyses of nucleophilic participation, such as that found for SpHex, indicates that the nucleophile interacts with a cationic center at the transition state. For SpHex it is quite reasonable to speculate, on the basis of considerable precedent with other glycosidases that use an *enzymic* nucleophile, that this cationic center is the sugar anomeric carbon in an oxocarbenium ion like transition state (*25*). Further studies, however, are required to verify this analogy.

Table 2: Kinetic Parameters for the Hydrolysis of a Series of Aryl Glucosaminides Catalyzed by SpHex and ExoII

substrate	phenol pK_a[a]	enzyme	k_{cat} (s^{-1})	K_m (mM)	k_{cat}/K_m (s^{-1} mM^{-1})
2,3DNPGlcNAc	4.96	ExoII	10.8 ± 0.2	0.09 ± 0.01	130 ± 10
(**5**)		SpHex	235 ± 9	0.019 ± 0.002	12000 ± 1000
3,5DNPGlcNAc	6.69	ExoII	4.8 ± 0.4	1.2 ± 0.1	4.0 ± 0.4
(**6**)		SpHex	222 ± 6	0.048± 0.005	4600 ± 500
pNPGlcNAc	7.18	ExoII	3.20 ± 0.04	0.73 ± 0.03	4.4 ± 0.2
(**7**)		SpHex	193 ± 3	0.049 ± 0.004	3900 ± 400
MuGlcNAc	7.50	ExoII	2.08 ± 0.08	1.2 ± 0.1	1.8 ± 0.1
(**8**)		SpHex	180 ± 7	0.054 ± 0.03	3300 ± 300
mNPGlcNAc	8.39	ExoII	0.33 ± 0.01	1.5 ± 0.1	0.22 ± 0.02
(**9**)		SpHex	197 ± 7	0.15 ± 0.03	1300 ± 100
pNHAcGlcNAc	9.50	ExoII	nd[b]	nd	nd
(**10**)		SpHex	206 ± 8	0.22 ± 0.01	940 ± 90
mNHAcGlcNAc	9.60	ExoII	0.054 ± 0.005	1.1 ± 0.1	0.05 ± 0.06
(**11**)		SpHex	187 ± 8	0.27 ± 0.04	700 ± 100
PGlcNAc	9.99	ExoII	0.012 ± 0.005	1.0 ± 0.1	0.011 ± 0.002
(**12**)		SpHex	172 ± 3	0.48 ± 0.01	360 ± 70

[a] pK_a values used for phenols were taken from refs *53*−*55*. [b] Not determined.

Charge Development on the Glycosidic Oxygen at the Transition State. Kosman and Jones (*18*) advanced a mechanistic proposal involving the formation of an exocyclic oxonium ion like transition state in which they suggest that the glycosidic oxygen is protonated very early in the reaction, perhaps even in the Michaelis complex (*18*). In such a transition state there would be very little fission of the glycosidic bond but nearly complete protonation of the glycosidic oxygen. Kosman and Jones rationalize this proposal on the basis of the small solvent isotope effect they observed ($k_H/k_D = 1.27$) during the *A. niger N*-acetylglucosaminidase-catalyzed hydrolysis of pNPGlcNAc (*18*). The small magnitude of this solvent isotope effect suggests that the proton is either almost completely transferred or hardly transferred to the glycosidic oxygen. These authors also argue that the small, slightly negative $\beta_{lg(k_{cat}/K_m)}$ value ($\beta_{lg} \approx -0.1$), determined from the *A. niger* β-*N*-acetylglucosaminidase-catalyzed hydrolysis of a series of four para-substituted 2-acetamido-2-deoxy-β-D-glucopyranosides, suggests little charge development on the glycosidic oxygen, thereby supporting their view. Consistent with their proposal are the observations that for the spontaneous and alkaline hydrolysis of glucosides the β_{lg} value is typically large and negative ($\beta_{lg} = -1$) while that observed for specific acid catalysis, where an oxonium ion is formed, is typically small and positive ($\beta_{lg} = 0.02$ to 0.2) (*17*). One alternative interpretation of the data of Jones and Kosman is that the transition state is more oxocarbenium ion like with advanced fission of the glycosidic bond as well as with significant proton donation. Indeed, such a late transition state is more consistent with the Taft-like analysis (vide supra) that indicates development of a positively charged center in the transition state. Furthermore, such a mechanism is consistent with the general catalytic mechanisms of β-retaining glycosidases (*31*).

To address this question we aimed to evaluate the extent of charge development at the glycosidic oxygen in order to establish whether, at the transition state, proton transfer was more or less advanced than cleavage of the glycosidic linkage. To this end we prepared a series of aryl *N*-acetylglucosaminides with varying leaving groups and tested these as substrates of both ExoII and SpHex (Figure 3). The kinetic parameters determined for each substrate with both enzymes are summarized in Table 2. These kinetic parameters can be plotted in a series of Brønsted linear free energy relationships (Figure 5), where several trends are seen.

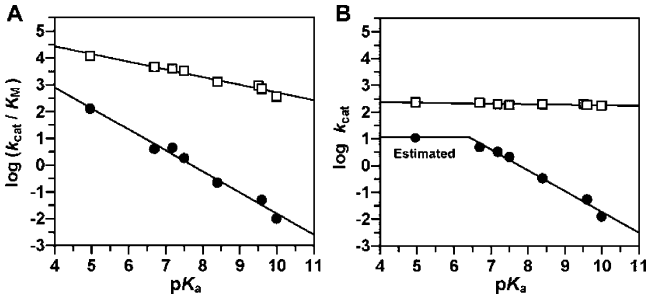

FIGURE 5: Brønsted plots of the log of the first (k_{cat}) and second (k_{cat}/K_m) order rate constants for the ExoII and SpHex hydrolysis of a series of aryl glucosaminide substrates. (A) Plot of log(k_{cat}/K_m) against the pK_a of the leaving group phenol. (B) Plot of log(k_{cat}) against the pK_a of the leaving group phenol. Filled circles (●) represent data for ExoII, and open squares (□) represent data for SpHex.

For ExoII the plot of log(k_{cat}/K_m) versus pK_a of the phenol leaving group shows a strong correlation for all substrates. The plot of log(k_{cat}) against the pK_a of the phenol leaving group also reveals a significant correlation but only for substrates bearing poor leaving groups with pK_a > 7. The values of $\beta_{lg(k_{cat})} = -0.78$ obtained from a linear regression of the data for all substrates other than 2,3DNPGlcNAc and the $\beta_{lg(k_{cat}/K_m)} = -0.79$ obtained from a linear regression of all the data are very similar. Indeed, identical slopes are expected if the rate-determining step, governed by k_{cat}, is also the first irreversible chemical step of the reaction, as governed by k_{cat}/K_m. The similarity of these two β_{lg} values suggests that the rate-determining step for these substrates (pK_a > 7) with ExoII is the glycosylation step. The deviation of 2,3DNPGlcNAc from the correlation of log(k_{cat}) presumably arises because the rate-determining step for this substrate with ExoII is the deglycosylation step. The relatively low K_m value that is found for 2,3DNPGlcNAc as compared to poorer substrates (pK_a > 7) supports this view. Low K_m values are often the consequence of accumulation of a glycosyl enzyme intermediate since K_m reflects the ratio of all enzyme bound species to free enzyme and substrate according to the following equation:

$$K_M = [E][S]/\sum[ES] \quad (1)$$

Although studies to substantiate this claim have not been carried out for ExoII, similar behavior has been observed with several retaining *exo*-β-glycosidases including, for example, β-glucosidases from sweet almonds (*32*), *Agrobacterium* sp. (*33*), and *Pyrococcus furiosus* (*34*), the β-mannosidase from *Cellulomonas fimi* (*35*), and the β-xylosidase from *Thermoanaerobacterium saccharolyticum* (*36*). The magnitudes of the β_{lg} values observed here for ExoII (-0.78 and -0.79) are also consistent with the studies listed above where β_{lg} values commonly lie between -0.7 and -0.95.

Linear regression analyses of the data obtained with SpHex for both $\log(k_{cat}/K_m)$ and $\log(k_{cat})$ values, as plotted against the pK_a values of the leaving group phenol, also yield good correlations throughout the entire range of substrates. This unbroken linear correlation suggests that the rate-determining step remains the same for all substrates. The markedly different $\beta_{lg(k_{cat})}$ (-0.02) and $\beta_{lg(k_{cat}/K_m)}$ (-0.29) values also indicate that the rate-determining step of the reaction, as reflected by k_{cat}, is not the first irreversible chemical step. Indeed, k_{cat} values show essentially no dependence on leaving group ability ($\beta_{lg(k_{cat})} \approx 0$), indicating that the rate-determining step is either the deglycosylation step or some nonchemical rate-determining step. A nonchemical rate-determining step is ruled out, however, by the α-deuterium kinetic isotope effect of significant magnitude (vide infra) measured on k_{cat} using pNPGlcNAc. The trend in K_m values also supports this proposal. As the leaving group becomes better, K_m decreases (Table 2), suggesting that the steady state concentration of an enzyme-sequestered intermediate is increasing. Presumably, this occurs as a consequence of an increased rate of cyclization relative to that of the ring-opening step, which must remain invariant regardless of the nature of the leaving group.

The magnitude of the $\beta_{lg(k_{cat}/K_m)}$ value measured for SpHex (-0.29) is greater that that estimated by Kosman and Jones from their four point study (-0.1) although the sign is the same in both studies. Both of these values are consistent with the $\beta_{lg(k_{cat}/K_m)}$ value of ≈ 0.2 we calculate by plotting a subset of the kinetic data reported by Tanaka et al. in their study of bovine liver β-*N*-acetylglucosaminidase (*37*). The small negative $\beta_{lg(k_{cat}/K_m)}$ (-0.29) observed with SpHex reflects the accumulation of a relatively small amount of negative charge on the glycosidic oxygen at the transition state of the glycosylation step and suggests that cleavage of the glycosidic bond is slightly, yet significantly, more advanced than is proton donation to the glycosidic oxygen. The negative β_{lg} values measured for both enzymes indicate that the glycosidic oxygen accumulates negative charge in the transition state, presumably as a consequence of the cleavage of the glycosidic bond. The difference in the magnitude of the $\beta_{lg(k_{cat}/K_m)}$ values between SpHex and ExoII hints either at a different requirement for acid catalysis in the two cases, or that cleavage of the glycosidic bond is more advanced in the first transition state of the reaction catalyzed by ExoII than it is for SpHex. If the difference is attributable to a varying requirement for acid catalysis, as we expect, proton donation is expected to play a more significant role in catalysis by the family 20 SpHex β-*N*-acetylglucosaminidase. A small negative β_{lg} value such as that seen for SpHex has been observed for a number of retaining β-glycosidases including the xylanase from *Cellulomonas fimi* (*38*) for which it has been established that bond cleavage is highly advanced. For SpHex, however, to unambiguously establish that the transition state for the SpHex-catalyzed reaction is more dissociative and oxocarbenium ion like than oxonium ion like, as suggested by Jones and Kosman, some measure of the geometry of the anomeric center at the transition state must be made.

α-*Deuterium Kinetic Isotope Effects.* A direct and rapid test to gain insight into the nature of the transition state is through the use of α-deuterium kinetic isotope effect (αD-KIE) studies. Indeed, such studies with LacZ β-galactosidase were the first to elegantly show that the glycosyl enzyme intermediate was, in fact, a covalent species rather than an intimately enzyme sequestered oxocarbenium ion (*39*). Furthermore, this approach was also used with the *C. fimi* xylanase that had a relatively small $\beta_{lg(k_{cat}/K_m)}$ value. Accordingly, for the family 20 β-*N*-acetylglucosaminidase SpHex, α-deuterium kinetic isotope effect studies should clarify whether the transition state is more oxonium ion like as suggested by Jones and Kosman (*18*), or more oxocarbenium ion like, as we expect. These studies may also provide unambiguous evidence pointing to whether the intermediates in the ExoII- and SpHex-catalyzed reactions are covalent species or stabilized oxocarbenium ions as is still sometimes posited. While it is generally accepted that most β-retaining glycosidases operate via a catalytic mechanism involving the transient formation of a *covalent* glycosyl enzyme intermediate, β-*N*-acetylglucosaminidases from family 20 are generally held to use a catalytic mechanism involving anchimeric assistance from the acetamido group of their substrates. This intermediate is thought to be either a bicyclic oxazoline intermediate (*5*, *6*, *40*) or, alternatively, a transient oxocarbenium ion intermediate that may be stabilized through close positioning of the acetamido group (*4*, *18*, *26*, *41*).

If the transition state is oxonium ion like, as postulated by Jones and Kosman, (*18*) with little C$-$O bond cleavage, then we expect that the αD-KIE will be approximately unity as the anomeric center will remain essentially sp^3 hybridized in both the starting material and the transition state. Conversely, if the transition state is oxocarbenium ion like with advanced fission of the C$-$O bond, then the hybridization of the anomeric center changes from sp^3 in the ground state to sp^2 in the transition state and, accordingly, a normal αD-KIE should be observed. In every case where such studies have been carried out, these kinetic isotope effects have been significantly greater than unity, revealing that the transition states leading to the formation and breakdown of a *covalent* glycosyl enzyme have considerable oxocarbenium ion like character (*25*). The only β-*N*-acetylglucosaminidase to have been investigated using αD-KIE studies is hen egg white lysozyme, which uses a catalytic mechanism involving a covalent glycosyl enzyme intermediate (*31*). In those studies a normal value of k_H/k_D of 1.14 was found for the first step of the reaction (*42*, *43*). No such studies have been carried out on any *exo*-β-*N*-acetylglucosaminidase from any family of glycoside hydrolases. On the basis of the Brønsted analyses it is clear that the rate-determining step for SpHex is deglycosylation (vide supra). If a significant and normal αD-KIE value is measured for k_{cat} with SpHex, we can infer that the intermediate is a covalent oxazoline intermediate. Last, in addition to clarifying these aspects of the mechanism of the family 20 β-*N*-acetylglucosaminidases these isotope

effects would provide further insight into the similarities and differences of the anchimeric assistance mechanism and the double displacement mechanism. To this end we prepared 1-{^{2}H}-pNPGlcNAc (**19**), which is isotopically enriched with deuterium at the anomeric center.

With the deuterium-labeled substrate in hand we sought to determine the αD-KIE values for both enzymes. Unfortunately, owing to the limited solubility of the substrate and the relatively high K_m value of this substrate for ExoII (K_m = 0.73 mM), saturating concentrations of substrate could not be reached and an $^{\alpha-D}(V)_{KIE}$ could therefore not be measured. The $^{\alpha-D}(V/K)_{KIE}$ value could, however, be measured for this enzyme. Conversely, for SpHex, the Michaelis constant is so small (K_m = 0.05 mM) as to make accurate spectrophotometric measurements by the substrate depletion method difficult. Therefore the isotope effect was measured under conditions of saturating substrate, yielding an $^{\alpha-D}(V)_{KIE}$ value for SpHex. As discussed above, k_{cat} values for SpHex likely reflect the deglycosylation step.

Since the cyclization and ring-opening steps are the near microscopic reverse of each other, however, these values provide some insight into the structures of the transition states for both steps. The isotope effect measured for SpHex ($k_H/k_D = 1.07 \pm 0.01$) reveals transition states having significant oxocarbenium ion character, as also suggested by the Taft-like analysis. The magnitude of this isotope effect also unambiguously establishes that the oxazoline intermediate is a covalent species and not a stabilized oxocarbenium ion as has been posited (*18*, *26*, *41*). The isotope effect measured for ExoII ($k_H/k_D = 1.10 \pm 0.02$) is very close to that measured for SpHex and suggests that the charge buildup at C-1 in the transition states of both enzymes is similar. These values are also within the range found for all retaining β-glycosidases studied to date (1.05−1.11 for the glycosylation step and 1.08−1.25 for the deglycosylation step) (*25*) and therefore support the idea of a common catalytic mechanism involving dissociative oxocarbenium ion like transition states bracketing a covalent intermediate for all of these enzymes regardless of the nature of the nucleophile. These results support the view that the intermediate in the catalytic pathway of any given retaining β-glycosidase may be either a covalent glycosyl enzyme or a covalent bicyclic oxazoline or oxazolinium ion (*31*, *44*).

CONCLUSION

Despite the difference in the identity and nature of the nucleophile, the transition states for both SpHex and ExoII appear remarkably similar. Cleavage of the glycosidic linkage is significantly advanced, with considerable charge development on the anomeric center as evidenced by the normal and significant α-deuterium kinetic isotope effects observed for both enzymes. Brønsted analysis of both enzymes also reveals that proton donation from the general acid/base catalytic residue lags behind cleavage of the glycosidic bond for both enzymes. For SpHex, proton donation appears more advanced, while for ExoII, proton donation lags far behind C−O bond fission. The consequence of these interpretations is that the transition state can be viewed as highly polar, with accumulation of net negative charge on the glycosidic oxygen and the −1 saccharide unit having significant oxocarbenium ion like character. These results are consistent with the very large majority of studies on retaining β-glycosidases and support the view that all retaining β-glycosidases, with the exception of the NAD-requiring enzymes of family 4 (*45*), use a fundamentally similar mechanism involving substrate distortion, general acid/base catalysis to facilitate the departure of the aglycon, and electrophilic migration of the anomeric center (*31*).

METHODS AND MATERIALS

General Procedures. All buffer chemicals and other reagents were obtained from the Sigma/Aldrich/Fluka Chemical Co. unless otherwise noted. Solvents and reagents used were either reagent, certified, or spectral grade. Anhydrous solvents were prepared as follows. Methanol was distilled from magnesium turnings in the presence of iodine; tetrahydrofuran was distilled from sodium in the presence of benzophenone; and toluene, pyridine, triethylamine, acetonitrile, and dichloromethane were prepared by distillation from calcium hydride. Solvents were distilled immediately prior to use. Dimethylformamide was dried sequentially over 4 Å molecular sieves.

Synthetic reactions were monitored by TLC using Merck Kieselgel 60 F254 aluminum-backed sheets (thickness 0.2 mm). Compounds were detected by ultraviolet light (254 nm) and/or by charring with 10% ammonium molybdate in 2 M H_2SO_4 and heating. Flash chromatography under a positive pressure was performed with Merck Kieselgel 60 (230−400 mesh) using the specified eluants. ^{1}H NMR spectra were recorded on a Bruker WH-400 spectrometer at 400 MHz, a Bruker AV-300 at 300 MHz, or a Bruker AC-200 at 200 MHz. ^{19}F NMR spectra were recorded on a Bruker AC-200 at 188 MHz or a Bruker AV-300 at 282 MHz and are proton-coupled with CF_3CO_2H as a reference. Chemical shifts are reported on the δ scale in parts per million from tetramethylsilane (TMS) and were measured relative to $CDCl_3$, CD_3OD, or to DSS when taken in D_2O. The abbreviations used in describing multiplicity are (s) singlet, (d) doublet, (t) triplet, (m) multiplet, and (br) broad. Carbon nuclear magnetic resonance (^{13}C NMR) spectra were obtained on a Varian XL-300 spectrometer at 75.5 MHz. Signal positions are given in parts per million (ppm) from tetramethylsilane and were measured relative to the signal of $CDCl_3$, CD_3OD, or D_2O. The Mass Spectrometry Laboratory, University of British Columbia, performed both high and low resolution mass spectra. Mr. Peter Borda of the Microanalytical Laboratory, University of British Columbia, performed elemental analyses. Melting points were recorded using a Laboratory Devices Mel-Temp II melting point apparatus and are uncorrected.

Synthesis. The syntheses of pNPGlcNAcF_2 (**3**) (*29*) and 2-deoxy-3,4,6-tri-*O*-acetyl-2-trifluoroacetamido-β-D-glucopyranosyl bromide (*46*) were performed as previously described.

*p-Nitrophenyl 2-Deoxy-3,4,6-tri-O-acetyl-2-trifluoroacetamido-β-D-glucopyranoside (**4**).* An alternative to the approach described in the literature (*29*) was chosen to prepare large quantities of this compound. Under an atmosphere of nitrogen, to a solution of 2-deoxy-3,4,6-tri-*O*-acetyl-2-trifluoroacetamido-β-D-glucopyranosyl bromide (3.48 g, 7.5 mmol) (*46*) in anhydrous acetonitrile (30 mL) was added $CaSO_4$ (2 g). To a different solution, also under an

atmosphere of nitrogen, containing 2,6-lutidine (1.86 mL, 18.8 mmol, 2.5 equiv) and *p*-nitrophenol (dried in vacuo overnight, 2.1 g, 15.1 mmol, 2 equiv) in anhydrous acetonitrile (30 mL) was added $CaSO_4$ (2 g). These two separate slurries were then stirred at room temperature for 30 min, after which time the mixture containing the phenol was cannulated into the flask containing the glycosyl bromide. Silver carbonate was added (1.32 g, 0.75 equiv) to the suspension, and the resulting mixture was stirred vigorously in the dark for 3 h, after which time TLC analysis revealed that the glycosyl bromide had entirely reacted. The reaction mixture was diluted with acetonitrile, and the solids were removed by filtration through a bed of silica and Celite. The filtrate was concentrated in vacuo to provide a gray gum. The desired product was then purified by flash chromatography on silica gel (ethyl acetate/hexanes; 1:1) to yield the desired product (**4**) (3.05 g, 5.9 mmol, 78%) as a crystalline solid. ^{1}H and ^{19}F NMR data for compound **4** can be found in Tables 1 to 5 of the Supporting Information.

General Synthesis of Aryl 2-Acetamido-2-deoxy-3,4,6-tri-O-acetyl-β-D-glucopyranosides. The phase-transfer method of Roy and Tropper (*47*) was followed. Briefly, to a mixture of 2-acetamido-2-deoxy-3,4,6-tri-*O*-acetyl-α-D-glucopyranosyl chloride (*48*) (1 equiv), tetrabutylammonium hydrogen sulfate (1 equiv), and the acceptor phenol (2 equiv) was added sufficient dichloromethane (1 volume) to yield a solution containing the donor chloride at a concentration of 200 mM. An equal volume of 1 M NaOH (1 volume) was then added, and this mixture was rapidly stirred at room temperature for 1 to 3 h. After the reaction was judged complete by TLC analysis, ethyl acetate (5 volumes) was added. The solution was washed with 1 M NaOH (4 × 2 volumes), water (2 × 2 volumes), and saturated sodium chloride solution (2 volumes). The organic layer was dried ($MgSO_4$) and filtered, and the solvent was removed in vacuo. The resulting crude product was crystallized from a mixture of ethyl acetate and hexanes to provide yields after 1 crop of between 45% and 70% of the desired aryl glycoside. ^{1}H NMR data for the per-acetylated aryl *N*-acetylglucosaminides can be found in Tables 1 to 5 of the Supporting Information. The per-acetylated derivatives of compounds **7** (*49*), **9** (*37*), **10** (*47*), and **12** (*37*, *47*) are known in the literature, and spectral data reported in the Supporting Information are consistent with the available data.

*General Synthesis of Aryl 2-Acetamido-2-deoxy-β-D-glucopyranosides (**1**−**4**, **5**−**12**, and **19**).* To a stirred solution of the aryl 2-acetamido-2-deoxy-3,4,6-tri-*O*-acetyl-β-D-glucopyranoside (per-acetylated derivative of compounds **1**−**4**, **5**−**12**, and **19**) in anhydrous methanol was added a catalytic amount (1−5 drops) of a 1 M solution of sodium methoxide in methanol. The reaction mixture was stirred for 2 to 4 h at room temperature. In cases where a precipitate formed, this was filtered and washed with methanol. The mother liquor of this reaction and all other reactions was processed in the same manner. Excess Amberlite IR-120 resin (H^+) was added, and the reaction mixture was filtered. The filtrate was concentrated in vacuo to provide a solid. Recrystallization of all compounds was accomplished using a mixture of methanol−ether−hexanes. Yields of the desired product after one recrystallization ranged from 30% to 75%. ^{1}H NMR data, melting points, and elemental analyses for compounds **1** to **4** and **5** to **12** can be found in Tables 1 to 5 of the Supporting Information. Compounds **7** (*49*), **9** (*37*), **10** (*47*), and **12** (*37*, *47*) are known in the literature, and spectral data reported in the Supporting Information are consistent with the available data. Elemental analyses of all compounds used in these studies are reported in the Supporting Information.

*1-{^{2}H}-2-Acetamido-2-deoxy-3,4,6-tri-O-benzyl-α/β-D-glucopyranose (**15**).* To a stirred solution of 3,4,6-tri-*O*-benzyl-D-glucono-1,5-lactone (**14**) (*50*) (9.7 g, 28 mmol) in anhydrous THF (130 mL) was added a solution of sodium borodeuteride (0.22 g, 5.2 mmol) in 0.99 mL of D_2O. The reaction mixture was stirred at room temperature for 2 h, after which time the reaction was judged complete by TLC analysis. The resulting solution was concentrated in vacuo to a pale yellow syrup, and dichloromethane (200 mL) was added. After the syrup had dissolved, the organic layer was washed with water (2 × 100 mL) and saturated sodium chloride solution (1 × 100 mL). The organic layer was dried over $MgSO_4$, concentrated in vacuo to a syrup, and crystallized from ethyl acetate−hexanes to provide a mixture of the title compounds as a white crystalline solid (82% yield, 8.0 g, 23 mmol). ^{1}H NMR (400 MHz, $CDCl_3$): 7.35−7.15 (15 H, m, Ph), 5.37 (1 H, d, $J_{NH,H2}$ = 8.8 Hz, NH), 4.86−4.76 (3 H, m), 4.68−4.48 (5 H, m), 4.11 (1 H, dd, $J_{H2,H3}$ = 10.3, H-2), 4.03 (1 H, ddd, $J_{H5,H4}$ = 9.7 Hz, $J_{H5,H6}$ = 4.8 Hz, $J_{H5,H6a}$ = 2.8 Hz, H-5), 3.80 (2 H, m), 3.68−3.60 (3 H, m), 1.81 (3 H, s, NAc).

*1-{^{2}H}-2-Acetamido-2-deoxy-α/β-d-glucopyranose (**16**).* The atmosphere of a solution of 1-{^{2}H}-2-acetamido-2-deoxy-3,4,6-tri-*O*-benzyl-β-D-glucopyranose (**15**, 1.2 g, 2.43 mmol) in a mixture of ethyl acetate and methanol (10 mL each) was replaced with nitrogen, and a catalytic amount of palladium on carbon was added. The atmosphere above the reaction was replaced with hydrogen, and the mixture was stirred for 16 h, at which time the reaction was judged by TLC analysis to be complete. The reaction mixture was filtered through glass fiber filter paper and concentrated in vacuo to yield a white powder (475 mg, 2.14 mmol, 88%). ^{1}H NMR (400 MHz, D_2O): 3.80−3.52 (4.7 H), 3.46−3.32 (1.3 H, m), 1.93 (3 H, s, NAc).

*1-{^{2}H}-2-Acetamido-2-deoxy-3,4,6-tri-O-acetyl-α-D-glucopyranosyl Chloride (**17**).* This compound was prepared essentially as described for the nondeuterated compound 2-acetamido-2-deoxy-3,4,6-tri-*O*-acetyl-α-D-glucopyranosyl chloride by Leaback (*48*).

*1-{^{2}H}-2-Acetamido-2-deoxy-β-D-glucopyranoside (**19**).* This compound was prepared as described above under the sections General Synthesis of Aryl 2-Acetamido-2-deoxy-3,4,6-tri-O-acetyl-β-D-glucopyranosides and General Synthesis of Aryl 2-Acetamido-2-deoxy-β-D-glucopyranosides.

Enzyme Kinetics with ExoII. All kinetic studies involving ExoII were performed in 50 mM sodium phosphate, 200 mM sodium chloride, pH 7.00, containing 0.1% bovine serum albumin. For each substrate a continuous spectrophotometric assay based on the rate of release of the phenolic leaving group upon hydrolysis of the chromogenic substrate was used. The resulting absorbance change was measured using a Pye-Unicam 8700 UV/vis spectrophotometer equipped with a circulating water bath set at 23.5 °C. The wavelengths monitored varied for each substrate and are listed in the Supporting Information. Michaelis−Menten parameters for the hydrolysis of all substrates by ExoII were determined by directly fitting the intial rate data to the Michaelis−

Menten equation using GraFit version 3.0 (*51*). The concentrations of enzyme and substrate used in each assay can be found in the Supporting Information.

Enzyme Kinetics with SpHex. SpHex was recombinantly expressed in *Escherichia coli* and purified essentially as outlined by Williams et al. (*21*). All kinetic studies involving SpHex were performed in 25/25 mM sodium citrate/sodium phosphate, 150 mM sodium chloride, pH 4.50. For each substrate a continuous spectrophotometric assay based on the rate of release of the phenolic leaving group upon hydrolysis of the chromogenic substrate was used. The resulting absorbance change was measured using a Pye-Unicam 8700 UV/vis spectrophotometer equipped with a circulating water bath at 37.0 °C. The wavelengths monitored varied for each substrate and are listed in the Supporting Information. Michaelis−Menten parameters for the hydrolysis of all substrates by SpHex were determined by directly fitting the intial rate data to the Michaelis−Menten equation using GraFit version 3.0 (*51*). The concentration of enzyme and substrate used in each assay can be found in the Supporting Information.

Kinetic Isotope Effects. Isotope effects using 1-{^{2}H}-pNPGlcNAc were determined in two different ways due to limitations arising from the K_m values with each enzyme and the limited solubility of the substrate. For ExoII the relatively high K_m value (K_m = 0.73 mM) prohibited measurement of the $^{\alpha-D}(V)$ isotope effect due to the limited solubility of the substrate. Thus for this ExoII the $^{\alpha-D}(V/K)$ isotope effect was determined by continuously monitoring the depletion of a low concentration of substrate ($^1/_{18}K_m$) in the reaction at 400 nm. For SpHex saturation conditions were readily obtained (K_m = 50 μM) and therefore $^{\alpha-D}(V)$ isotope effects were determined. An accurate determination of the $^{\alpha-D}(V/K)$ isotope effect for SpHex was precluded by the low concentration of substrate required (0.1K_m to 0.2K_m) for these experiments and the consequent poor signal-to-noise in the progress curves. The standard assay conditions were used as described above except that for the experiments involving ExoII the concentration of 1-{^{2}H}-pNPGlcNAc was 70 μM and for SpHex a concentration of 1.2 mM was used. The reaction was initiated by the addition of an aliquot (20 μL) of thermally equilibrated substrate. Initial rates or second order rate constants were measured alternately for protio and deuterio samples until at least 8 rates for each had been determined. Average rates or rate constants were then calculated for the protio and deuterio substrates, and the ratio was taken to yield the isotope effect. ^{1}H NMR analysis of the sample of 1-{^{2}H}-pNPGlcNAc used showed that the extent of isotopic incorporation was >95%.

Determination of the Delta Absorption Coefficient ($\Delta\epsilon_n$) for Aryl Glycoside Substrates. A series of three or four solutions containing varying concentrations of the intact glycoside of interest were made up in quartz cells in the assay buffer for SpHex (vide supra). The absorption of these solutions at the appropriate wavelength was measured and the data were fitted by linear regression. In all cases the data revealed excellent linear correlations ($r \geq 0.99$) providing the extinction coefficient of the intact glycoside. SpHex (10 μL, 1.2 mg/mL) was added and the reaction allowed to proceed for 6 h, after which time the absorbance of each reaction mixture was again measured at the appropriate wavelength. The reaction was then allowed to proceed overnight, and the absorbance of each solution was again recorded. These absorbance readings were in close agreement with the readings taken the previous day, indicating that the reactions had been complete after 6 h. These data were fitted by linear regression using the program GraFit 3.0 (*51*), and in all cases the data revealed excellent linear correlations (r = 0.97) furnishing the extinction coefficient of the liberated phenol. The absorbance of the enzyme at each wavelength was also recorded. The extinction coefficient of the intact aryl glycoside of interest was subtracted from the extinction coefficient of the corresponding phenol and of the enzyme to provide the delta absorption coefficient ($\Delta\epsilon_n$).

ACKNOWLEDGMENT

Prof. Saul Roseman generously provided the plasmid bearing the ExoII gene. The plasmid bearing the SpHex gene was provided by Drs. Brian Mark and Michael James at the University of Alberta. pNPGlcNAcF and reference samples of $pNPGlcNAcF_2$ and $pNPGlcNAcF_3$ were generously provided by Dr. Tom Harvey. 2,4DNPGlc was generously provided by Dr. David Zechel.

SUPPORTING INFORMATION AVAILABLE

Tables of characterization of compounds used in this study including elemental analyses and ^{1}H NMR data as well as extinction coefficients of the compounds used in the assays and the assay conditions including enzyme concentrations and the wavelengths monitored during the assays. This material is available free of charge via the Internet at http://pubs.acs.org.

REFERENCES

1. Henrissat, B., and Bairoch, A. (1993) *Biochem. J. 293*, 781−788.
2. Henrissat, B., and Bairoch, A. (1996) *Biochem. J. 316*, 695−696.
3. Vocadlo, D. J., Mayer, C., He, S., and Withers, S. G. (2000) *Biochemistry 39*, 117−126.
4. Tews, I., Perrakis, A., Oppenheim, A., Dauter, Z., Wilson, K. S., and Vorgias, C. E. (1996) *Nat. Struct. Biol. 3*, 638−648.
5. Knapp, S., Vocadlo, D., Gao, Z., Kirk, B., Lou, J., and Withers, S. G. (1996) *J. Am. Chem. Soc. 118*, 6804−6805.
6. Mark, B. L., Vocadlo, D. J., Knapp, S. K., Triggs-Raine, B. L., Withers, S. G., and James, M. N. G. (2001) *J. Biol. Chem. 276*, 10330−10337.
7. Drouillard, S., Armand, S., Davies, G. J., Vorgias, C. E., and Henrissat, B. (1997) *Biochem. J. 328*, 945−949.
8. Legler, G., Roeser, K. R., and Illig, H. K. (1979) *Eur. J. Biochem. 101*, 85−92.
9. Withers, S. G., Warren, R. A. J., Street, I. P., Rupitz, K., Kempton, J. B., and Aebersold, R. (1990) *J. Am. Chem. Soc. 112*, 5887−5889.
10. Wicki, J., Rose, D. R., and Withers, S. G. (2002) *Methods Enzymol. 354*, 84−105.
11. Amaya, M. F., Watts, A. G., Damager, I., Wehenkel, A., Nguyen, T., Buschiazzo, A., Paris, G., Frasch, A. C., Withers, S. G., and Alzari, P. M. (2004) *Structure (Cambridge) 12*, 775−784.
12. Yang, J., Schenkman, S., and Horenstein, B. A. (2000) *Biochemistry 39*, 5902−5910.
13. Watts, A. G., Damager, I., Amaya, M. L., Buschiazzo, A., Alzari, P., Frasch, A. C., and Withers, S. G. (2003) *J. Am. Chem. Soc. 125*, 7532−7533.
14. Piszkiewicz, D., and Bruice, T. C. (1967) *J. Am. Chem. Soc. 89*, 6237−6243.
15. Piszkiewicz, D., and Bruice, T. C. (1968) *J. Am. Chem. Soc. 90*, 2156−2163.
16. Capon, B. (1969) *Chem. Rev. 69*, 4637−4644.
17. Capon, B. (1971) *Biochimie (Paris) 53*, 145−149.
18. Jones, C. S., and Kosman, D. J. (1980) *J. Biol. Chem. 255*, 11861−11869.
19. Yamamoto, K. (1974) *J. Biochem. (Tokyo) 76*, 385−390.

20. Legler, G., and Bollhagen, R. (1992) *Carbohydr. Res. 233*, 113−123.
21. Williams, S. J., Mark, B. L., Vocadlo, D. J., James, M. N., and Withers, S. G. (2002) *J. Biol. Chem. 277*, 40055−40065.
22. Mark, B. L., Mahuran, D. J., Cherney, M. M., Zhao, D., Knapp, S., and James, M. N. (2003) *J. Mol. Biol. 327*, 1093−1109.
23. Maier, T., Strater, N., Schuette, C. G., Klingenstein, R., Sandhoff, K., and Saenger, W. (2003) *J. Mol. Biol. 328*, 669−681.
24. Prag, G., Papanikolau, Y., Tavlas, G., Vorgias, C. E., Petratos, K., and Oppenheim, A. B. (2000) *J. Mol. Biol. 300*, 611−617.
25. Davies, G., Sinnott, M. L., and Withers, S. G. (1998) in *Comprehensive Biological Catalysis* (Sinnott, M. L., Ed.) Vol. 1, pp 119−208, Academic Press, New York.
26. Papanikolau, Y., Prag, G., Tavlas, G., Vorgias, C. E., Oppenheim, A. B., and Petratos, K. (2001) *Biochemistry 40*, 11338−11343.
27. Mark, B. L., Wasney, G. A., Salo, T. J., Khan, A. R., Cao, Z., Robbins, P. W., James, M. N., and Triggs-Raine, B. L. (1998) *J. Biol. Chem. 273*, 19618−19624.
28. Chitlaru, E., and Roseman, S. (1996) *J. Biol. Chem. 271*, 33433−33439.
29. Yamamoto, K. (1973) *J. Biochem. (Tokyo) 73*, 749−753.
30. Macauley, M. S., Whitworth, G. E., Debowski, A., Chin, D., and Vocadlo, D. J. (2005) *J. Biol. Chem. 280*, 25313−25322.
31. Vocadlo, D. J., Davies, G. J., Laine, R., and Withers, S. G. (2001) *Nature 412*, 835−838.
32. Dale, M. P., Kopfler, W. P., and Byers, L. D. (1986) *Biochemistry 25*, 2522−2529.
33. Kempton, J. B., and Withers, S. G. (1992) *Biochemistry 31*, 9961−9969.
34. Bauer, M. W., and Kelly, R. M. (1998) *Biochemistry 37*, 17170−17178.
35. Zechel, D. L., Reid, S. P., Stoll, D., Nashiru, O., Warren, R. A., and Withers, S. G. (2003) *Biochemistry 42*, 7195−7204.
36. Vocadlo, D. J., Wicki, J., Rupitz, K., and Withers, S. G. (2002) *Biochemistry 41*, 9727−9735.
37. Tanaka, M., Kyosaka, S., and Sekiguchi, Y. (1976) *Chem. Pharm. Bull. (Tokyo) 24*, 3144−3148.
38. Tull, D., and Withers, S. G. (1994) *Biochemistry 33*, 6363−6370.
39. Sinnott, M. L., and Souchard, I. J. L. (1973) *Biochem. J. 133*, 89−98.
40. Kobayashi, S., Kiyosada, T., and Shoda, S.-I. (1997) *Tetrahedron Lett. 38*, 2111−2112.
41. Terwisscha van Scheltinga, A. C., Armand, S., Kalk, K. H., Isogai, A., Henrissat, B., and Dijkstra, B. W. (1995) *Biochemistry 34*, 15619−15623.
42. Smith, L. E. H., Mohr, L. H., and Raftery, M. A. (1973) *J. Am. Chem. Soc. 95*, 7497−7500.
43. Dahlquist, F. W., Rand-Meir, T., and Raftery, M. A. (1969) *Biochemistry 8*, 4214−4221.
44. Mark, B. L., Vocadlo, D. J., Zhao, D., Knapp, S., Withers, S. G., and James, M. N. (2001) *J. Biol. Chem. 276*, 42131−42137.
45. Yip, V. L., Varrot, A., Davies, G. J., Rajan, S. S., Yang, X., Thompson, J., Anderson, W. F., and Withers, S. G. (2004) *J. Am. Chem. Soc. 126*, 8354−8355.
46. Wolfrom, M. L., and Conigliaro, P. J. (1971) *Carbohydr. Res. 20*, 369−374.
47. Roy, R., and Tropper, F. D. (1991) *Can. J. Chem. 69*, 817−821.
48. Leaback, D. H., and Walker, P. G. (1961) *Biochem. J. 78*, 151−156.
49. Leaback, D. H., and Walker, P. G. (1957) *J. Chem. Soc.* 4754−4760.
50. Granier, T., and Vasella, A. (1998) *Helv. Chim. Acta 81*, 865−880.
51. Leatherbarrow, R. J. (1996) *GraFit 3.09b*, Erithacus Software Ltd., Staines, U.K.
52. Hansch, C., and Leo, A. (1979) *Substituent constants for correlation analysis in chemistry and biology*, pp 1−339, Wiley, New York.
53. Barlin, G. B., and Perrin, D. D. (1961) *Q. Rev., Chem. Soc. 20*, 75−101.
54. Kortum, G., Vogel, W., and Andrussow, K. (1961) *Pure Appl. Chem. 1*, 450.
55. Robinson, R. A., Davis, M. M., Paabo, M., and Bower, V. E. (1960) *J. Res. Natl. Bur. Stand., Sect. A 64*, 347−347−352.

BI051121K